ADVANCED OPTICAL MATERIALS
www.advopticalmat.de

Visible Diffraction from Graphene and Its Application in Holograms

Haider Butt, Piran R. Kidambi, Bruno Dlubak, Yunuen Montelongo, Ananta Palani, Gehan A. J. Amaratunga, Stephan Hofmann, and Timothy D. Wilkinson*

A fundamental study of visible diffraction effects from patterned graphene layers is presented. By patterning graphene into optical gratings, visible diffraction from graphene is experimentally measured as a function of the number of layers and visible wavelengths. A practical application of these effects is also presented, by demonstrating an optical hologram based on graphene. A high resolution (pixel size 400 nm) intensity hologram is fabricated which, in response to incident laser light, generates a visible image. These findings suggest that visible diffraction in graphene can find practical application in holograms and should also be considered during the design and characterisation of graphene-based optical applications.

1. Introduction

Graphene, a single layer of carbon atoms and the basic building block for graphitic materials of all other dimensions, has been the focus of an enormous amount of research in recent years.[1,2] It is a new class of material offering remarkable properties for low-dimensional physics. Due to its interesting electrical and optical properties, a myriad of photonics and optoelectronics applications have been reported, such as the utilisation of graphene as transparent and flexible electrodes in photovoltaic/solar cells,[3,4] light-emitting devices,[5] and photodetectors.[6] In addition, graphene is also being considered as a potential replacement for transparent electrodes in liquid-crystal-based display devices.[7]

In such optical modulating devices, in addition to the electrical conductance and optical transmission characteristics of graphene, visible diffraction also becomes a crucial factor. Graphene-based patterned electrodes have been recently utilised in touch-screen devices.[8,9] In these devices, the visible diffraction from graphene electrodes may lead to blurring of the display screens. Hence, it is vital to study the optical diffraction properties of monolayer and few-layer graphene.

Although substantial research has been done so far towards studying the visible transmission and absorption of graphene,[10–12] no literature exists which reports the diffraction of visible light from graphene. Here, we present a fundamental study both experimentally measuring and practically applying the visible diffraction from single- and multi-layered graphene. Patterned samples of graphene are used to experimentally measure its diffraction efficiency. We also demonstrate a diffractive hologram based on patterned graphene. This is the world's thinnest hologram (of the order of ~2 nm) ever used for projecting a visible and intelligible image.

Dr. H. Butt
School Mechanical Engineering
University of Birmingham
Birmingham B15 2TT, UK
E-mail: hb319@cam.ac.uk
Tel: 0044 1223 748320; Fax: 0044 1223 748322
Dr. H. Butt, Dr. P. R. Kidambi, Dr. B. Dlubak,
Y. Montelongo, A. Palani, Prof. G. A. J. Amaratung, Dr. S. Hofmann,
Prof. T. D. Wilkinson
Electrical Engineering Division
Department of Engineering
University of Cambridge
Cambridge CB3 0FA, UK
Prof. G. A. J. Amaratung
Sri Lanka Institute of Nanotechnology (SLINTEC)
Lot 14, Zone A, EPZ, Biyagama, Sri Lanka

DOI: 10.1002/adom.201300320

2. Synthesis of the Graphene

For studying the diffraction from graphene, monolayer graphene was synthesized using a low-pressure chemical vapour deposition (LPCVD) process on commercially available cold-rolled Cu foils (Alfa Aesar Puratronic, 99.999% purity, 25 μm thick), as described in detail elsewhere.[13] Post synthesis, the monolayer graphene was transferred to SiO_2 (300 nm)/Si substrates using a poly(methyl methacrylate) (PMMA) support layer and a 0.5 M aqueous solution of $FeCl_3$ to etch the Cu foil.[13] The PMMA support layer was removed using acetone, followed by a rinse in isopropanol.[13] Bi- and tri-layer graphene samples were synthesized by stacking monolayer graphene by repeated transfer.

Figure 1a shows an optical image of large-area monolayer graphene transferred to the SiO_2(300 nm)/Si wafer substrate. The corresponding Raman spectrum in Figure 1b (measured using a Renishaw InVia spectrometer using 532 nm laser) shows the characteristic intensity (I) peaks for graphene, i.e., 2D (~2700 cm^{-1}), G (~1600 cm^{-1}), and D (~1350 cm^{-1}) peaks. The 2D peak can be fitted with a single Lorentzian curve and $I_{2D}/I_G > 2$ and $I_D/I_G \sim 0.06$ confirms monolayer graphene of high quality.[13]

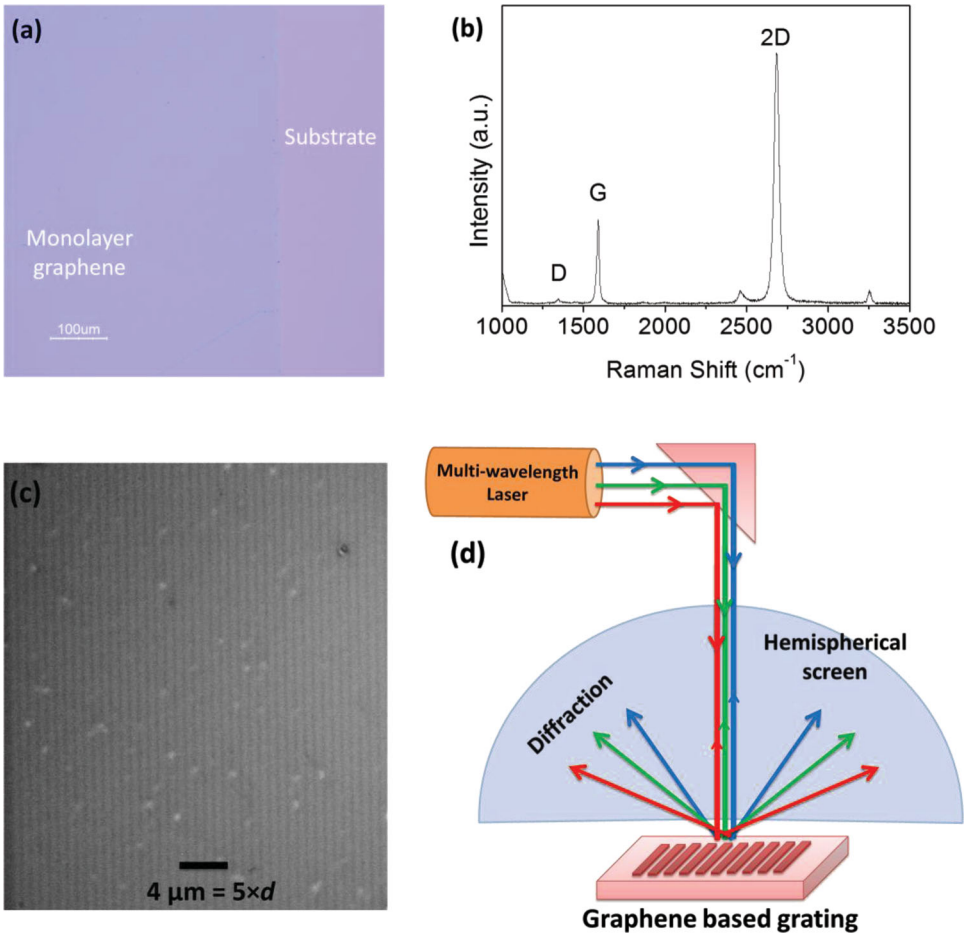

Figure 1. (a) Optical image and (b) Raman spectrum for the synthesized monolayer graphene transferred to a SiO_2 (300 nm)/Si wafer. (c) Optical image of a patterned optical grating based on a tri-layer graphene sample. The grating has a pitch of d = 800 nm. (d) The experimental setup used to record the visible diffraction from graphene-based optical gratings. A semi-transparent hemispherical screen (radius 40 mm) was used for viewing the diffracted light.

3. Graphene-Based Gratings

The synthesized graphene layers were patterned into gratings (Figure 1c) to study the visible diffraction from them. Gratings (and later holograms) were defined on graphene layers by an e-beam lithography step using a PMMA resist. After resist development, exposed graphene surfaces were etched by an O_2 plasma, resulting readily in a millimetre-scale patterned graphene layer. As shown in Figure 1c, the pitch d of the optical grating was set to 800 nm (with each strip only 400 nm wide), which is on the order of the wavelength of visible light. In accordance with Bragg diffraction, a pitch d = 800 nm will allow the diffraction of the visible light at large angles, simplifying the optical measurements.

Figure 1d shows the schematic diagram of the optical setup used for measuring the diffraction efficiency of graphene. A multi-wavelength laser was used to illuminate the graphene samples, at normal incidence. The samples were illuminated with blue, green, and red lasers with respective wavelengths of 445 nm, 532 nm, and 650 nm. The multi-wavelength laser source produced well aligned and collimated laser beams of each colour with an average power of 5 mW. When the laser beam was shone on the graphene gratings, a major portion of light was reflected back into the zero-order (undiffracted light) and a fraction was diffracted. The far field diffraction pattern produced by the optical grating consists of two symmetric spots (**Figure 2**). The diffracted spots were captured on a semi-transparent hemispherical screen of radius 40 mm.

Figure 2 shows the visible diffraction patterns produced when 1-, 2-, and 3-layered graphene samples were illuminated with blue, green, and red lasers. The diffraction in response to blue laser was the weakest and the most difficult to image. Therefore, an extended camera exposure time was used. The response to the green laser was the most clear and undistorted. It is also observed that, with the increase in wavelength, the diffraction angles of the spots increased. In accordance with the Bragg equation $\lambda = d \sin\theta$, where λ is the wavelength and θ is the diffraction angle, the light from blue, green, and red lasers will be diffracted at angles of the order of 34, 42, and 54 degrees to the normal.

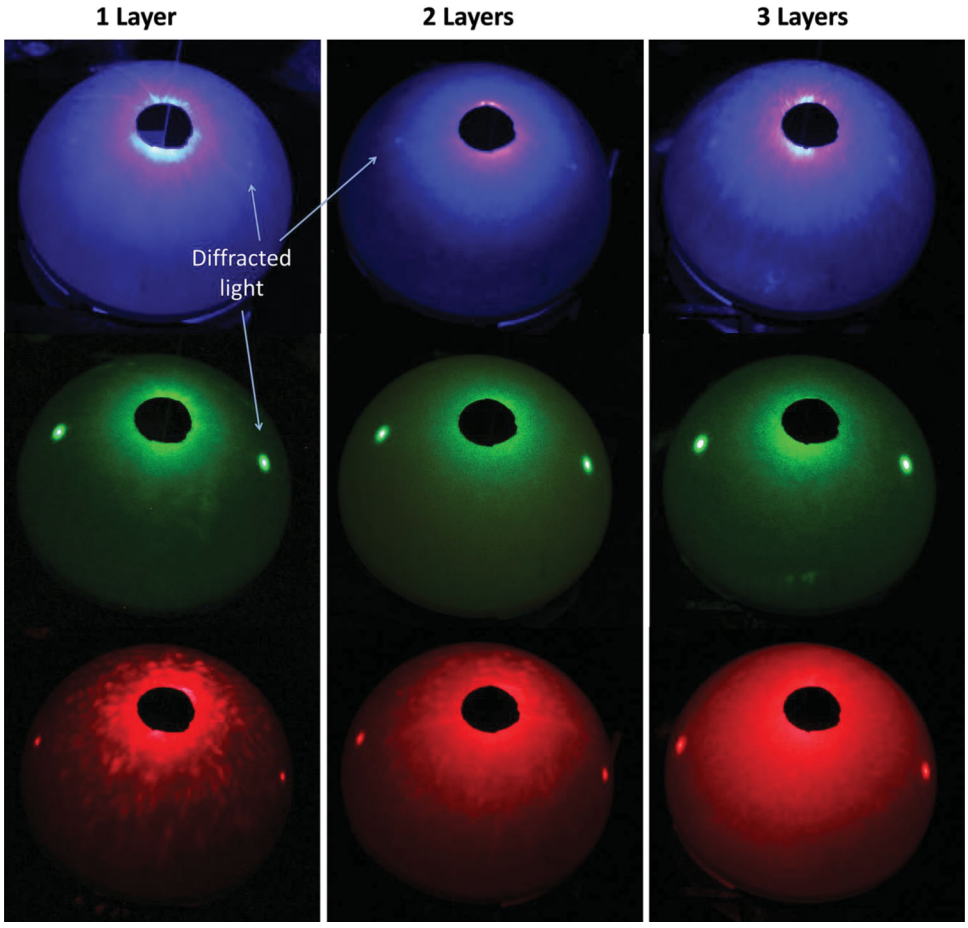

Figure 2. Visible diffraction from graphene-based optical gratings. The experiments were performed on 1-, 2-, and 3-layered graphene samples. Each sample was illuminated with red, blue, and green lasers. Two symmetric diffraction spots were observed on a semi-transparent hemispherical screen of radius 40 mm. The angle of diffracted light increased with laser wavelength.

4. Diffraction Efficiency Measurements

The experimental setup was also used to measure the visible diffraction efficiency from graphene as a function of the number of layers and the wavelength. Measurements were performed using two calibrated power meters adjusted to the wavelength of the given laser from a three-coloured laser system, where one power meter measured the light reflected 20 cm perpendicular to the sample surface and the second measured the angular diffracted light 3 cm from the sample surface. The samples were placed on an XY-translation stage that allowed a given sample position to be adjusted until the patterned graphene region was directly under the laser. The sample was tilted slightly off-perpendicular from the illuminating laser so that the reflected light did not follow the same path as the laser light, which would interfere with the measurements.

Measurements of the reflected energy from an unpatterned area of the graphene were taken relative to the SiO_2/Si substrate, as shown in **Figure 3**a. All measurements were repeated to check for consistency. The reflection efficiency of unpatterned graphene decreased for the red and blue lasers with increasing numbers of layers. However, the reflectivity for the green laser increased with the increasing number of layers. This is due to the increased contrast that is displayed by graphene on SiO_2 (300 nm)/Si substrates for green light. The 300 nm high SiO_2 layer on the Si substrate acts as a Fabry–Pérot cavity and the resonant wavelength undergoes an enhanced transmission while the non-resonant waves are reflected. Our simulation results (see the Supporting Information) suggest that with the increase in the number of graphene layers the effective height of SiO_2 layer-based cavity increases. This leads to a redshift in the resonant cavity modes, causing enhanced reflection for the green laser light. However, we emphasize that the main focus of the paper is to characterise the diffraction properties of graphene.

Since the diffraction pattern produced by the graphene grating comprising a spot and its complement, the diffraction efficiency is simply twice the power from a single spot relative to the undiffracted light in the zero order. The remaining energy was either absorbed by the sample or diffracted in undesirable ways due to surface irregularity, diffraction pattern imperfections, or contamination by dust and PMMA residuals. The power meter measuring diffraction energy had a sensing area of 1 cm^2, whereas the diffracted spot size had a diameter of approximately 1 mm. This was not a problem for the red and green laser lights, which seemed to cause very little undesirable diffraction. However, for the blue laser, the diffraction noise

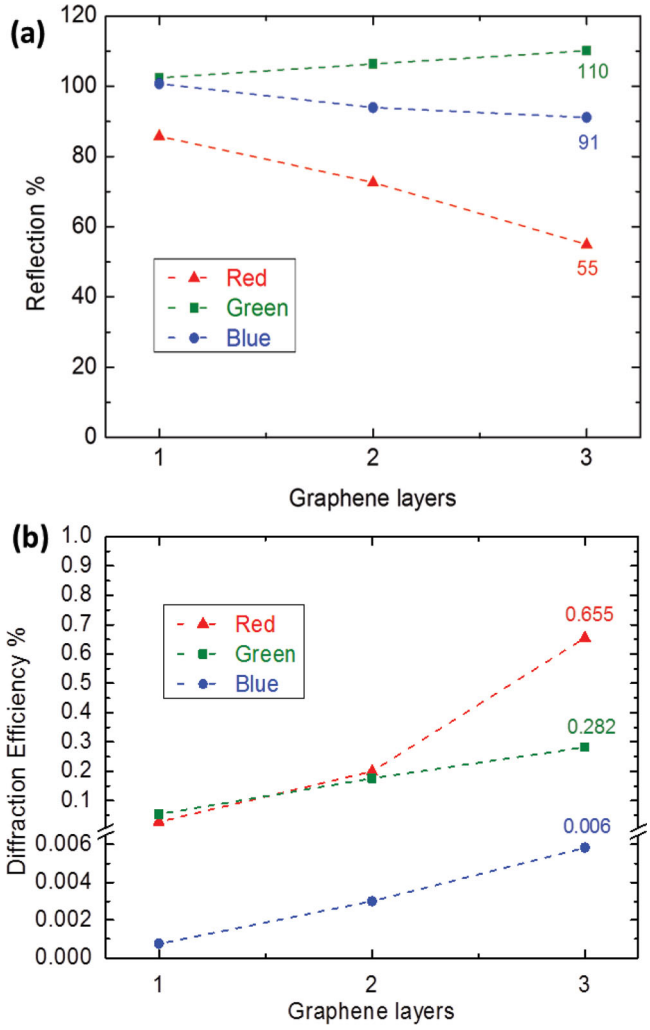

Figure 3. (a) Percentage reflection from unpatterned graphene layers relative to SiO_2/Si substrates. (b) Measured diffraction efficiency as a function of wavelength and the number of layers.

was quite high (due to the laser imperfections) and a mask over the power meter sensor was used with only a small hole, slightly larger than the diffraction spot size, in order to differentiate the spot from the noise. Measurements were performed with this mask for all laser colours (Figure 3b).

The diffraction efficiency measurements in Figure 3b show a clear trend of increasing efficiency with the increasing number of layers and wavelength. Visible absorption for graphene increases with the increasing number of layers,[10] which leads to an increased efficiency of the graphene-based optical grating. The diffracted efficiency for blue light was the least, at about 0.006% for three layers of graphene. For less than six layers, graphene does not contribute towards the phase modulation of light and only acts as an amplitude modulator.[14,15] Despite being only an atom thick, graphene has a considerably high optical absorption (~2.3%)[10,16] and, according to recent reports, the absorption can be further increased by doping graphene.[17] An increased absorption can further enhance the diffraction efficiency of patterned graphene. This is due to the increase in intensity between the light reflected from the regions with and without graphene.

The diffraction efficiency of graphene-based gratings will also be affected by the substrates used. Here, the choice of SiO_2/Si substrates seemed natural since graphene is clearly visible to the naked eye when placed on 300(nm) SiO_2/Si substrates.[10] This enabled easy cross-checks of the patterns after e-beam lithography under a normal optical microscope. Hence, the diffraction from graphene was studied in reflection mode. Further, the diffraction effects are possibly enhanced by the Fabry–Pérot cavity response produced by the 300 nm-high SiO_2 layer. We note that, on glass substrates, without the cavity effect the diffraction efficiency might be weaker and could be studied in transmission mode.

The performance of optical applications utilising patterned graphene as transparent electrodes might be affected by the diffraction effects.[8] In display devices, graphene electrodes would be patterned into micrometer-sized gratings which, according to the Bragg equation, will produce optical diffraction at small angles with the normal (on the order of 0 to 10 degrees). This may lead to the blurring of the display screens. The severity of the effect will be increased by several parameters, including the decrease in the period of the patterned gratings, the number of graphene layers used, and the total number of patterned electrodes. For instance, devices consisting of two patterned graphene electrodes will have almost twice the diffraction-based blurring effect, with a diffraction efficiency of approximately 1%.

5. A Graphene-Based Hologram

The measurements on graphene-based gratings show that the diffraction of visible light can be achieved from graphene layers. To demonstrate this effect in the form of a practical application, a graphene-based diffractive hologram was designed. In this unique and original endeavour we aimed to establish an ultrathin hologram consisting of a few atomic layers of graphene to project an engineered image. A graphene-based hologram was conceptualized as an intensity (amplitude) mask that, in response to light, produces a pattern in the far field similar to a Fraunhofer hologram (**Figure 4**). The hologram consisted

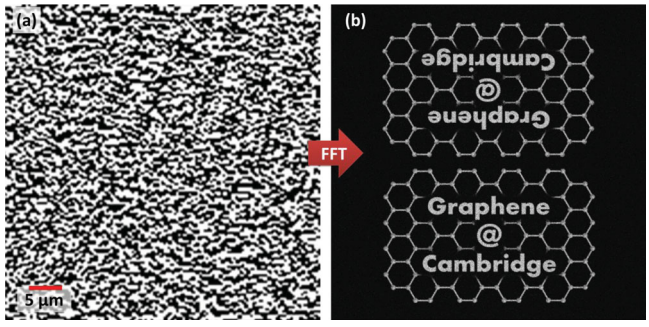

Figure 4. Calculation results for the 2D holographic pattern. (a) A cropped image of the calculated 2D hologram based on a 1000 × 1000 array of square pixels. The length of each pixel was 400 nm. (b) 2D Fourier transform of the whole array producing a diffraction pattern consisting of symmetric "Graphene @ Cambridge" images. The zero order was removed from the image for proper viewing.

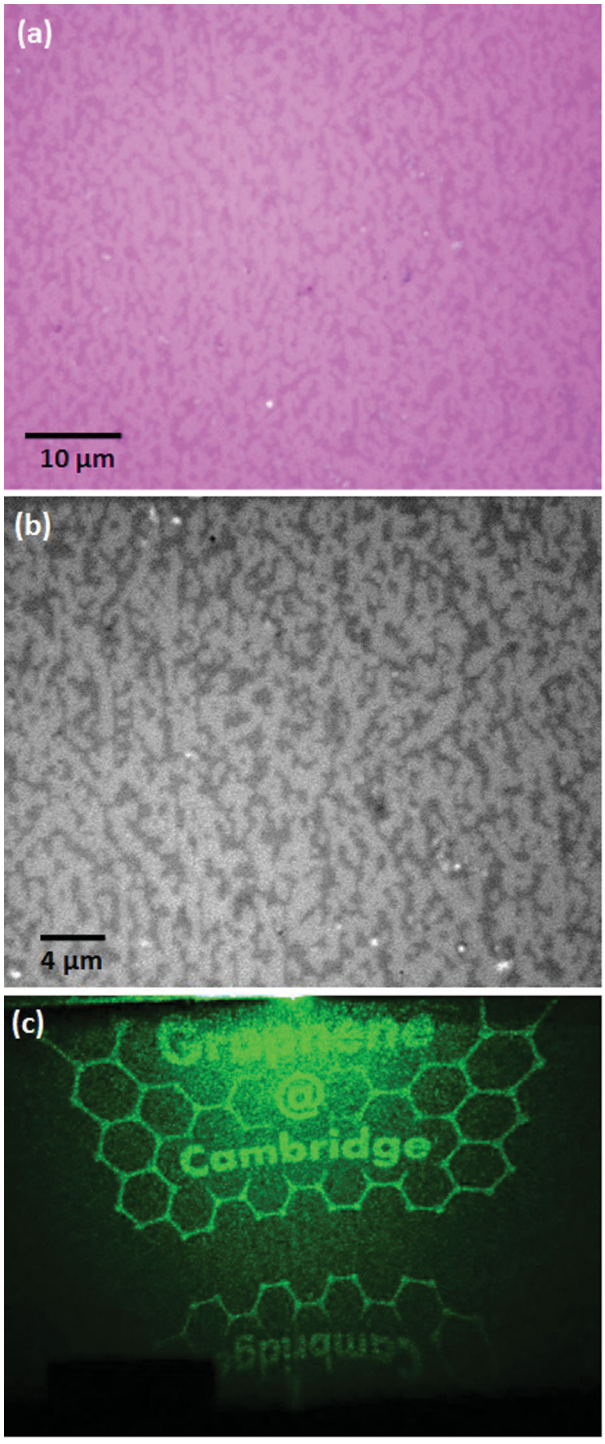

Figure 5. (a) Optical microscope image of a patterned 3-layer graphene sample. (b) A higher-resolution greyscale image of the same. The holographic pattern consisted of square pixels of length 400 nm. (c) The holographic image produced when the patterned graphene sample is illuminated with a green laser beam.

of a binary intensity mask whose Fourier transform produces an arbitrary image.[18] Here, the hologram consisting of 1000 × 1000 square pixels was designed to produce a far-field image saying "Graphene @ Cambridge".

The size of each pixel was set to 400 nm to get a wide field-of-view image. In order to optimize the hologram, a Gerchberg–Saxton algorithm was applied. To give a physical shape to the hologram, the array of deltas representing the hologram was convolved with geometrical shape in every delta (square). Figure 4a shows a section of the optimized solution of the hologram and Figure 4b the simulated far-field diffraction pattern (the image). According to the Fourier theory, a binary intensity hologram always reconstructs an image with its corresponding complex conjugated.

Using the sample fabrication method described above, graphene-based holograms were synthesized and patterned. **Figure 5**a shows the fabricated holograms based on patterned 3-layer graphene. In order to test the hologram, it was illuminated by a 5 mW green laser and the reflected image was viewed on a screen placed at a distance of around 20 cm. A green laser was used as, according to the measured results in Figure 1, it produced the most clear and visually simple-to-capture diffraction effects from graphene. The resulting diffracted image produced is shown in Figure 5c. A good agreement between the simulated and experimentally obtained holographic images was obtained. Our study serves as a practical demonstration of a potential application of the diffraction effects produced from patterned graphene. We note, however, that the measured performance is not comparable to commercially available holographic devices.

6. Conclusion

The results suggest that diffractive effects from graphene can be used in practical device applications (holograms). These effects can be enhanced by doping graphene to increase absorption and also by integrating them with a tuneable media like liquid crystals. While graphene acts as patterned electrodes modulating the amplitude of light, liquid crystals can perform complementary phase modulation to achieve workable holographic devices. Also, our measurements on graphene-based gratings highlight the qualitative visible diffraction from various graphene layers.

Supporting Information

Supporting Information is available from the Wiley Online Library or from the author.

Acknowledgements

H. Butt and P. R. Kidambi contributed equally to this work. This work was supported by EPSRC EP/K016636/1. H. Butt thanks Cambridge Philosophical Society and Wolfson College Cambridge for the research fellowship.

Received: August 1, 2013
Revised: August 20, 2013
Published online: October 9, 2013

[1] A. K. Geim, K. S. Novoselov, *Nat. Mater.* **2007**, *6*, 183–191.
[2] F. Bonaccorso, Z. Sun, T. Hasan, A. C. Ferrari, *Nat. Photonics* **2010**, *4*, 611–622.
[3] X. Wang, L. Zhi, K. Mullen, *Nano Lett.* **2008**, *8*, 323–327.

[4] L. Gomez De Arco, Y. Zhang, C. W. Schlenker, K. Ryu, M. E. Thompson, C. Zhou, *ACS Nano* **2010**, *4*, 2865–2873.
[5] P. Matyba, H. Yamaguchi, G. Eda, M. Chhowalla, L. Edman, N. D. Robinson, *ACS Nano* **2010**, *4*, 637–642.
[6] F. Xia, T. Mueller, Y. Lin, A. Valdes-Garcia, P. Avouris, *Nat. Nanotechnol.* **2009**, *4*, 839–843.
[7] P. Blake, P. D. Brimicombe, R. R. Nair, T. J. Booth, D. Jiang, F. Schedin, L. A. Ponomarenko, S. V. Morozov, H. F. Gleeson, E. W. Hill, A. K. Geim, K. S. Novoselov, *Nano Lett.* **2008**, *8*, 1704–1708.
[8] K. S. Kim, Y. Zhao, H. Jang, S. Y. Lee, J. M. Kim, K. S. Kim, J.-H. Ahn, P. Kim, J.-Y. Choi, B. H. Hong, *Nature* **2009**, *457*, 706–710.
[9] S. Bae, H. Kim, Y. Lee, X. Xu, J.-S. Park, Y. Zheng, J. Balakrishnan, T. Lei, H. Ri Kim, Y. I. Song, Y.-J. Kim, K. S. Kim, B. Özyilmaz, J.-H. Ahn, B. H. Hong, S. Iijima, *Nat. Nanotechnol.* **2010**, *5*, 574–578.
[10] R. R. Nair, P. Blake, A. N. Grigorenko, K. S. Novoselov, T. J. Booth, T. Stauber, N. M. R. Peres, A. K. Geim, *Science* **2008**, *320*, 1308–1308.
[11] L. Yang, *Phys. Rev. B* **2010**, *81*, 155445.
[12] P. A. Obraztsov, M. G. Rybin, A. V. Tyurnina, S. V. Garnov, E. D. Obraztsova, A. N. Obraztsov, Y. P. Svirko, *Nano Lett.* **2011**, *11*, 1540.
[13] P. R. Kidambi, C. Ducati, B. Dlubak, D. Gardiner, R. S. Weatherup, M.-B. Martin, P. Seneor, H. Coles, S. Hofmann, *J. Phys. Chem. C* **2012**, *116*, 22492–22501.
[14] C. Casiraghi, A. Hartschuh, E. Lidorikis, H. Qian, H. Harutyunyan, T. Gokus, K. S. Novoselov, A. C. Ferrari, *Nano Lett.* **2007**, *7*, 2711–2717.
[15] M. Bruna, S. Borini, *Appl. Phys. Lett.* **2009**, *94*, 031901.
[16] S. P. Apell, G. W. Hanson, C. Hägglund, arXiv:1201.3071v1 [physics. optics] http://arxiv.org/abs/1201.3071, **2012**.
[17] L. Yang, *Nano Lett.* **2011**, *11*, 3844–3847.
[18] H. Butt, Y. Montelongo, T. Butler, R. Rajesekharan, Q. Dai, S. G. Shiva-Reddy, T. D. Wilkinson, G. A. J. Amaratunga, *Adv. Mater.* **2012**, *24*, OP331–OP336.